

Numerical Analysis of a Long Bridge with Tall Piers under simultaneous action of Seismic Excitation and Moving Train

Abhishek, Post Graduate Student, Civil Engng. Dept., IIT Guwahati, India

Prinza Priya Loying, Sumantra Sengupta, Research Scholar, Civil Engng. Dept., IIT Guwahati, India

and Dr. Anjan Dutta, Professor, Civil Engng. Dept., IIT Guwahati, India

Abstract

The study is related to the assessment of performance of a long multi-span railway bridge with through type open web superstructure and located in the highest seismic zone of India under simultaneous action of earthquake and moving train. Piers are tall with heights varying from 60 to 140 m and are expected to show significant amplification of seismic response at pier top level. In a long bridge, spatial variation in the input seismic excitation should be considered; **the effect of this variation at different pier foundation levels on the overall seismic performance of the bridge must be assessed.** A detailed finite element model with soil-structure interaction is considered. Asynchronous ground motions are modelled using conditional simulation that accounts for the coherency losses and a time delay of arrival with change in phase as well as amplitude of the earthquake signals from origin to the spatial points of interest along the bridge. Multi-support excitation of the bridge is performed by converting the acceleration time history to displacement time history. A 27 DOF vehicle model is used to assess the safety of a moving train, while the bridge is simultaneously acted upon by an earthquake shaking. The responses at different pier locations for the synchronous and asynchronous motion are evaluated, and the requirement of asynchronous input in multi-support excitation for a long bridge with tall piers is observed to be significant for the assessment of safety of running vehicle.

Keywords

Long bridge with tall piers, Seismic performance, Conditional Simulation, Asynchronous motion, multi-support excitation, Vehicle model

1. Introduction

Long bridges may have multiple supports and the abutments at two ends as well as intermediate piers, are quite likely to be at a significant distance apart. During seismic excitation, the expectation of the same earthquake motion at every support point is thus unlikely to be accurate, as during its propagation, the earthquake motion undergoes reflection, refraction, and losses its coherent nature, resulting in a whole different motion when measured at different points for the same earthquake event.

The spectral properties of ground motion get altered because of (a) wave passage effects which is due to the time shifts in the arrival of the seismic waves at the supports (Adanur et al.[1]) (b) the incoherence effect which is due to extended source effect in which different frequencies in the relative geometry of the source and site produce different time shift (Konakli and Kiureghian [2]) (c) the local soil effect which causes scattering (reflection, refraction etc) of waves by inhomogeneity along the travel path. The asynchronous ground motions were started being analyzed after the installation of dense instrument arrays since 1979 with El Centro differential arrays. Before this, the spatial variation of the motions was attributed to the wave propagation effect only (Bogdanoff et al. [3]).

Numerous researchers have done work on spatial variation of seismic ground motion and its application on long span structures. In general, the spatial variations of seismic ground motions are evaluated from data recorded at dense instrument arrays. Zerva and Zervas [4] studied the estimation of coherency from the recorded data and discussed on its interpretation. Some empirical and semi-empirical coherency models based on the recorded data, their validity as well as limitations and the effect of coherency on the seismic response of extended structures were studied. Lavorato et al. [5] studied the nonsynchronous seismic ground motion generated at different foundation point of a long span bridge. Basu et al. [6] developed a framework which accounts for both phase variability and amplitude variability of spatially varying ground motion. For assessment, a definition of target spectrum based on the direction of arrival was explored. The effect of choice of coherency model on the simulated spatially varying ground motion was investigated. ("Practical coherency model suitable for near- and far-field earthquakes ...") Seismic response analysis of structures subject to multi-support excitation has been carried out by various methods like modal analysis (Berrah [7]), modified response spectrum method (Kiureghian and Neuenhofer [8]), Monte Carlo simulation (Mirzabozorg et al. [9]), random vibration analysis (Zhang et al. [10]), etc. Balamonoca et al.[11] used a deterministic approach using proper orthogonal decomposition vector (POD) or proper orthogonal mode to analyse the response of the structure subjected to multisupport excitation. Experimental and numerical studies show that the relative displacement of the bridges tends to increase, causing pounding when subjected to spatially varying earthquakes (Li et al.[12]). Nguyen et al. [13] established a simulation procedure for vehicle-substructure dynamic interactions. Each vehicle is modelled as a multi-axle double-layer of a mass-spring-damper system having 27 DOFs, and the bridge is modelled using the finite element method. The wheel-rail dynamic interaction model couples the train subsystem with the track subsystem at the wheel-rail interfaces.

rigid contact assumption, where the wheel displacement is considered identical to that of the bridge or rail beneath it, implying continuous contact without separation (Yang et al. [14]) has been popularly used by many researchers.

It is understood from the literature study that the asynchronous motion will cause enhanced relative motion in pier top in multi support long span bridge compared to synchronous motion. In railway bridge, this effect causes relative displacement of the continuous rail on which trains are moving. "In the present study, development of asynchronous motion and its effect on long span bridge with multi support arrangement has been presented." ("Civil-Comp Conference Proceedings") In railway bridge, the continuous track alignment undergoes lateral movement during seismic excitation. The train speed depends on the track curvature in addition to the other factors. The relative effect of track curvature between synchronous and asynchronous ground movement has been studied for a long railway bridge with tall piers and located in the highest seismic zone of India. A 27 DOF vehicle model with rigid contact assumption has been considered in the present study. The seismic performance of bridge-vehicle system has been studied to examine the importance of synchronous and asynchronous ground movement in terms of safety of the overall system.

2. Finite Element Modelling of the Considered Bridge

The bridge under consideration is a railway bridge with an open web girder superstructure. The bridge is in Manipur, India, which has the highest seismicity in the country. The total length of the considered bridge is 703 m, which comprises of eight simply supported spans. It has two 69 m span with a through-type truss girder, five numbers of 103.5 m span with a through-type truss girder and a plate girder span of 28.5 m. The bridge consists of seven intermediate annular piers of height ranging from 60 metres to 141 metres.

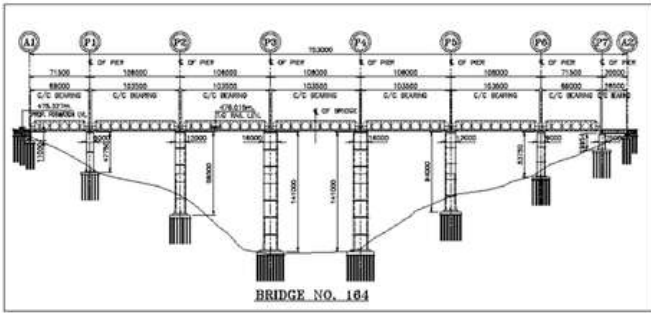


Fig. 1 Tall Long Railway Bridge in Manipur

The tall Piers resting on Pile foundations are flexible and must be modelled appropriately to represent their actual behaviour. The bridge is supported on a group of piles with a diameter of 1.5 meters and a length varying between 22 meters to 30 meters at the respective locations (Figure 1). Members of the superstructure with different sectional geometries are modelled in section designer. Beam elements are used to model the piers, piles, while plate elements are used to model the pile cap. The superstructure is also modelled using beam elements, wherein appropriate releases are made to ensure only axial degrees of freedom to members of the truss and rotational degrees of freedom are released for stringers and cross girders to ensure shear transfer only. The through-type truss girder and plate girder spans are simply supported, and boundary conditions are imposed with help of body constraints in SAP 2000 Nonlinear. The near-field soil is modelled using Beam on Winkler Foundation, where soil elements are modelled as discrete non-linear springs as specified in API 2008 [15]. The soil resistance in the lateral and axial direction of the pile is summarised as a P-y curve to represent the relationship between the lateral resistance of soil and pile displacement, a t-z curve to represent the relationship between shaft skin frictional force and relative movement of the pile with respect to the soil, Q-z curve to represent the mobilized tip bearing capacity and settlement. "The detailed finite element model of the considered bridge, along with the soil-pile system, is shown in Fig. 2 ("Civil-Comp Conference Proceedings")

3. Multi-Support Excitations Using the Displacement Input Method

Multi-support excitation in SAP 2000 Nonlinear is performed by converting acceleration time history to displacement time history, while the time step is reduced to 1/10th of acceleration time history.

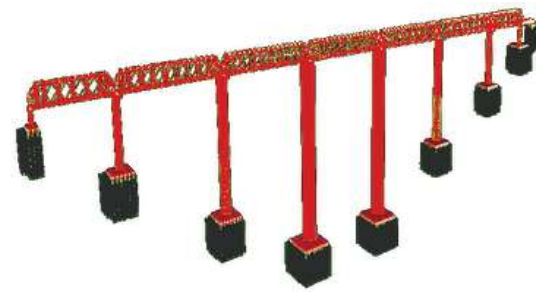


Fig. 2 Finite Element Model of the Bridge with Near-Field Soil Springs

The P-y spring is positioned along with two orthogonal directions on the horizontal plane and is connected to the pile at discrete points over its length. The converted displacement time history and applied as joint/ground displacement at each fixed end of the two-jointed P-y spring (Fig. 3).

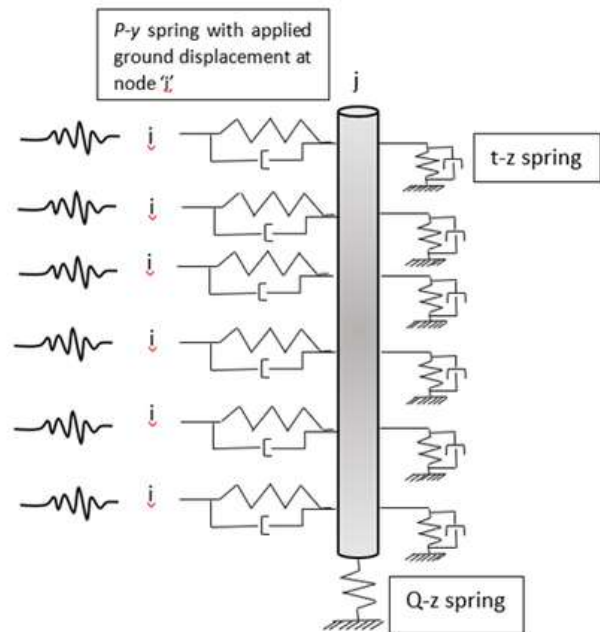


Fig. 3 Schematic diagram of Pile with input ground displacement at i^{th} node

The structural response that is obtained from displacement-based input is the total displacement response, whereas for acceleration-based input, the response that is obtained is the relative displacement response. The equations of motions that are solved by SAP 2000 for performing multi-support excitation are:

$$\begin{bmatrix} M_{ss} & M_{sb} \\ M_{sb} & M_{bb} \end{bmatrix} \begin{pmatrix} \ddot{u}_s \\ \ddot{u}_b \end{pmatrix} + \begin{bmatrix} C_{ss} & C_{sb} \\ C_{sb} & C_{bb} \end{bmatrix} \begin{pmatrix} \dot{u}_s \\ \dot{u}_b \end{pmatrix} + \begin{bmatrix} k_{ss} & k_{sb} \\ k_{sb} & k_{bb} \end{bmatrix} \begin{pmatrix} u_s \\ u_b \end{pmatrix} = \begin{pmatrix} 0 \\ R_b \end{pmatrix} \quad (1)$$

where, $\ddot{u}_s, \dot{u}_s, u_s$ are the vectors representing the motion of the superstructure in the absolute coordinate system; $\ddot{u}_b, \dot{u}_b, u_b$ are the vectors representing ground motion in the absolute coordinates;

M_{ii} , C_{ii} , k_{ii} are the mass, damping and stiffness matrices. The meaning of subscripts like ss, bb and sb is the degrees of freedom of the superstructure, base, and their coupled term. R_b is the lateral reaction at the nodes of the foundation. Considering the expanded form of the first row of Equation 1, we get

$$M_{ss}\ddot{u}_s + C_{ss}\dot{u}_s + k_{ss}u_s = -(M_{sb}\ddot{u}_b + C_{sb}\dot{u}_b + k_{sb}u_b) \quad (2)$$

In the case of the lumped mass model, all non-diagonal terms are zero, thus M_{sb} is equal to zero. The damping term $-C_{sb}\dot{u}_b$ can be neglected (Computers and Structures [16]). So, Equation 2 can be written as

$$M_{ss}\ddot{u}_s + C_{ss}\dot{u}_s + k_{ss}u_s = -k_{sb}u_b \quad (3)$$

where u_b is the vector of ground motion in terms of displacements; $-k_{sb}u_b$ is the force experienced by the superstructure for the ground motion in the absolute coordinates. Equation 3 is the displacement-based input model for the analysis of a structure under ground motion.

4. Vehicle Model

In this study, the train model considered comprises of a locomotive and wagons. The number of wagons is chosen in such a way that a large part of the bridge remains loaded. The car body has a total of 5

degrees of freedom (DOFs): vertical, lateral, rolling, yawing and pitching. Similarly, both the front and the rear bogies are assigned 5 DOFs each, while the four-wheel sets of the vehicle are assigned 3 DOFs each. Thus, the 3D vehicle model of the wagon has 27 DOFs. The vehicle model along with the axle spacing and loads are shown in Fig.4 (Nguyen et al. [13]).

The rigid contact algorithm adopted in this study is based on the formulation proposed by Yang et al. [14].

5. Seismic Analysis of the Long Span Bridge for Synchronous and Asynchronous Input Motion

In the present study, two earthquake records with different peak accelerations, frequency contents and durations have been selected as input motion for the time-history analysis of the considered bridge. These recorded earthquakes are Koyna (1967): Comp – Longitudinal and Elcentro (1940): 180-degree component. These input earthquake motions have been converted to a spectrum compatible with respect to the design spectrum for DBE (5% damped) as presented in IS: 1893 [15]. These spectrum compatible time histories are used as synchronous input motion. The conditional simulation of earthquakes that vary spatially using the procedure that has been developed by Fenton et al. [16] is adopted in this study and is used as asynchronous input motion.

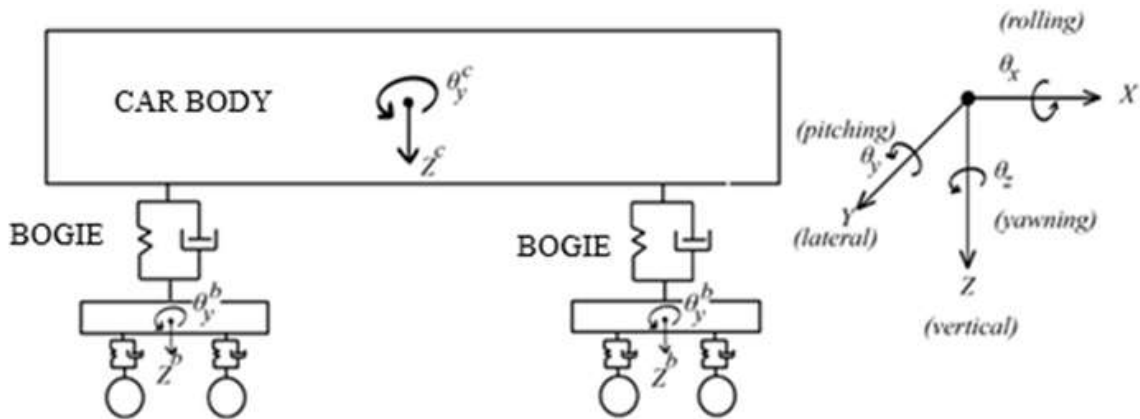


Fig. 4 Vehicle Model with 27 Degrees of Freedom

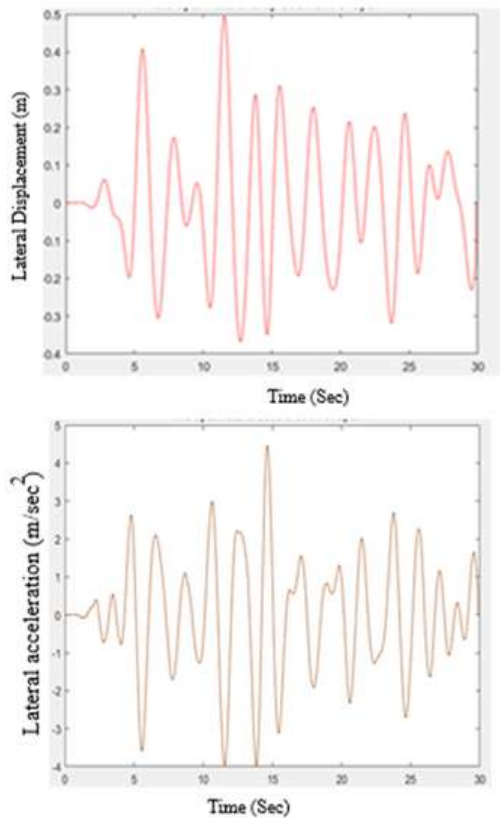


Fig. 5 Lateral displacement and acceleration of span P2-P3 under Elcentro excitation with no train on bridge

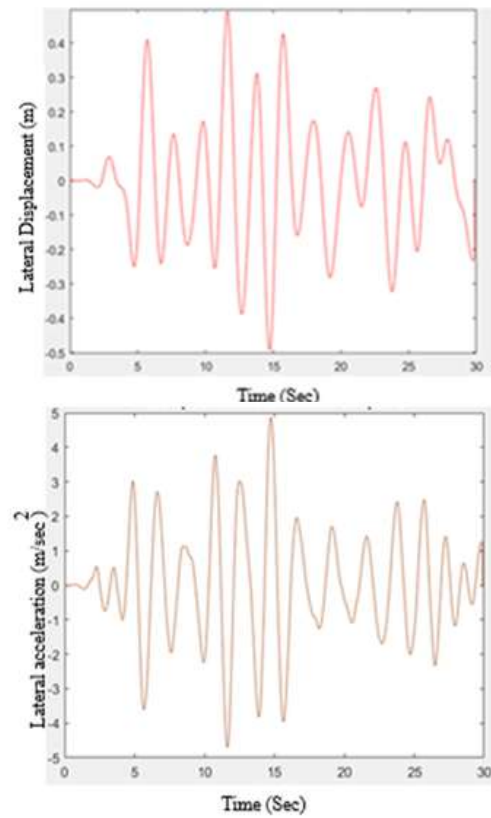


Fig. 6 Lateral displacement and acceleration of span P3-P4 under Elcentro excitation with no train on bridge.

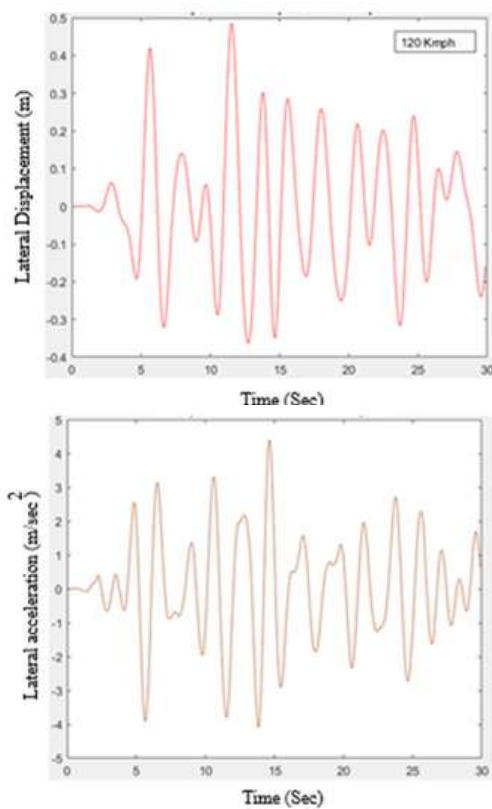


Fig. 7 Lateral displacement and acceleration of span P2-P3 under Elcentro excitation with train moving at 120 kmph.

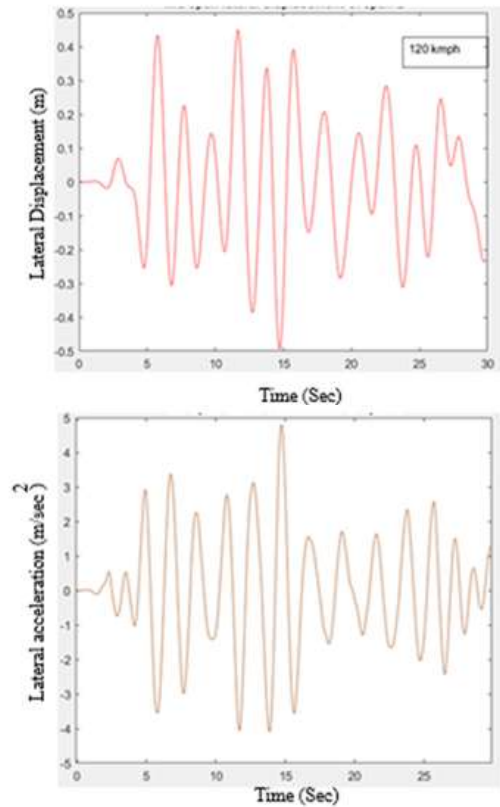


Fig. 8 Lateral displacement and acceleration of span P3-P4 under Elcentro excitation with train moving at 120 kmph.

5.1 Comparison of Responses at Pier Top

The maximum response value at the bridge mid span for different velocities of train for both the cases is shown in Table-1. A few typical time history plots of lateral acceleration and displacement of the bridge at mid span are shown in figures 5-8. It is observed that the bridge structure with a train shows a lesser response in comparison to the case where there is no train and the structure is subjected to seismic excitation alone.

Table 1 Response of Bridge Under Elcentro Excitation for Various Cases

Elcentro Earthquake					
Response at mid span	Span no.	No train condition	With train		
			Speed of train (kmph)		
			60	80	120
Lateral displacement(m) (Synchronous)	P3-P4	0.5049	0.4895	0.4923	0.4955
	P2-P3	0.4930	0.4898	0.4903	0.4919
Lateral displacement (m) (Asynchronous)	P3-P4	0.4587	0.4483	0.4512	0.4529
	P2-P3	0.4326	0.4283	0.4298	0.4310
Lateral acceleration (m/s ²) (Synchronous)	P3-P4	4.4648	4.3720	4.3941	4.3971
	P2-P3	4.8687	4.8175	4.8517	4.8532
Lateral acceleration (m/s ²) (Asynchronous)	P3-P4	4.1693	4.0289	4.1092	4.1461
	P2-P3	4.3278	4.2434	4.2473	4.3048

In the present analysis, span 2 exhibits the highest lateral displacement, which may be attributed to the greater height of pier 2 and pier 3, resulting in increased flexibility. Furthermore, the absolute response under synchronous excitation is observed to be higher than in the asynchronous case.

Table 2 Response of bridge under Mexico earthquake for various cases

Mexico Earthquake					
Response at mid span	Span no.	No train condition	With train		
			Velocity of train (kmph)		
			60	80	120
Lateral displacement (m) (Synchronous)	P3-P4	0.4236	0.4147	0.4212	0.4234
	P2-P3	0.3907	0.3850	0.3897	0.3902
Lateral displacement (m) (Asynchronous)	P3-P4	0.3855	0.3779	0.3818	0.3846
	P2-P3	0.3390	0.3311	0.3340	0.3369
Lateral acceleration (m/s ²) (Synchronous)	P3-P4	4.3113	4.1274	4.2025	4.2514
	P2-P3	4.8925	4.8019	4.8468	4.8902
Lateral acceleration (m/s ²) (Asynchronous)	P3-P4	3.9498	3.8717	3.885	3.9161
	P2-P3	4.4164	4.3219	4.3866	4.4054

5.2 The relative displacement of adjacent piers

The bridge under study exhibits geometric irregularity due to varying pier heights. Pier-2(P2) and Pier-3(P3), both measuring 98 m and 141 m respectively, are connected by a 103.5-meter span. Under synchronous excitation, these piers tend to vibrate in phase, resulting in minimal relative displacement between them. However, when asynchronous ground motion is considered, the excitation reaches the piers at various times, leading to significant relative displacement that is not captured in the synchronous case. This increased relative movement can potentially cause unseating of girders from their supporting bearings, posing a risk to structural integrity. The relative displacement of P2 and P3 is shown in Figure 9 for asynchronous Elcentro excitation.

As observed from the analysis, asynchronous ground motion results in increased relative displacement between adjacent piers of the bridge. This differential movement arises due to the time lag and spatial

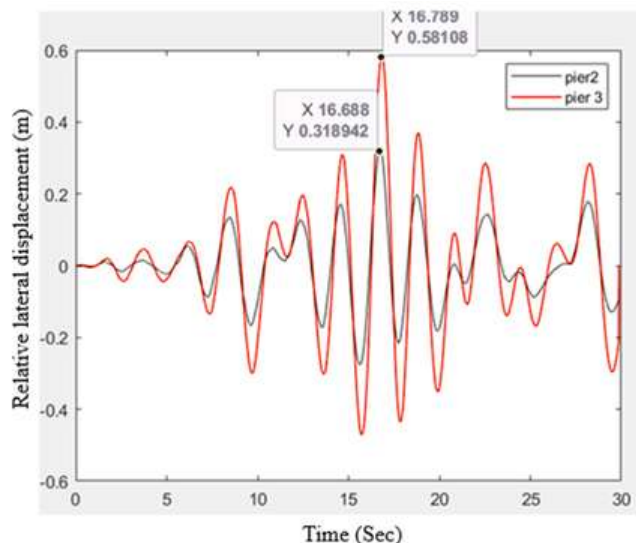


Fig. 9 Relative displacement between Pier 2 (P2) and Pier 3 (P3)

variation in seismic wave arrival, especially significant in long-span bridges or those with varying pier heights. Such increased relative displacement can introduce irregularities in the track alignment, potentially leading to misalignment or even damage to the continuous welded rail system. These irregularities pose a serious threat to the stability and safety of high-speed or trains with higher axle loads operating during or immediately after an earthquake. Therefore, considering asynchronous seismic effects is essential for the accurate assessment of track-structure interaction and the overall seismic safety of railway bridges.

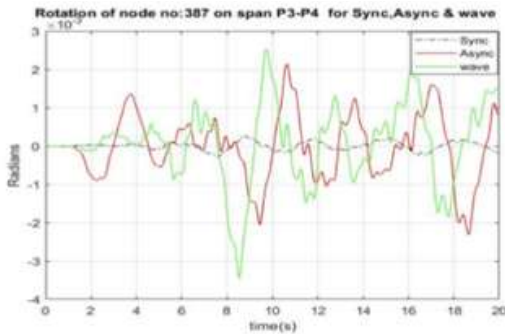
5.3 Other significant observations

The input motion with wave passage effect and coherency losses can introduce significant variation in responses of some degree of freedom, which are otherwise observed to have negligible values under synchronous motion as input. A few superstructure nodes, such as node number 387 on span P3-P4

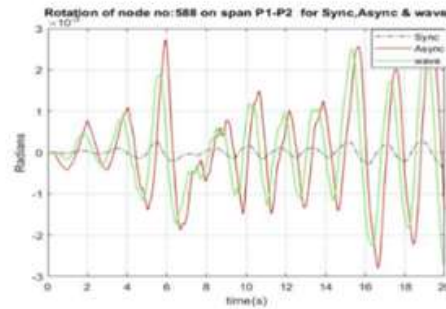
case. Similar observations were also made by Balamonica et al. [11] that the torsional degree of freedom is underestimated in analysis with synchronous input and may cause significant torsional stresses in the superstructure.

5.4 Effect on track curvature

The curvature of the deflected track under transverse seismic ground movement has been studied for the Elcentro EQ and Koyna EQ, for both synchronous and asynchronous motion. In Figure 9 (a-b), the curvature of the deflected track has been plotted along the length of the bridge at different time instances when the individual pier top deflection is maximum. Two such deflected track alignments corresponding to synchronous and asynchronous transverse ground movement, considering El-Centro and Koyna EQ, have been plotted and shown in Figure 10 (a-b) at the time instance when the deflection at the top of pier P3 is maximum. All the deflections are absolute, and the considered points have been joined by a spline to



(a) At node 387 on span P3-P4

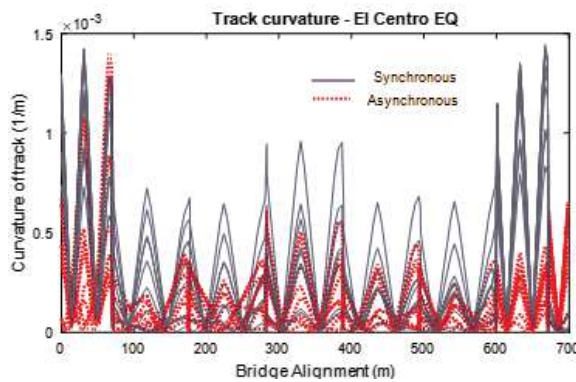


(b) At node 588 on span P1-P2

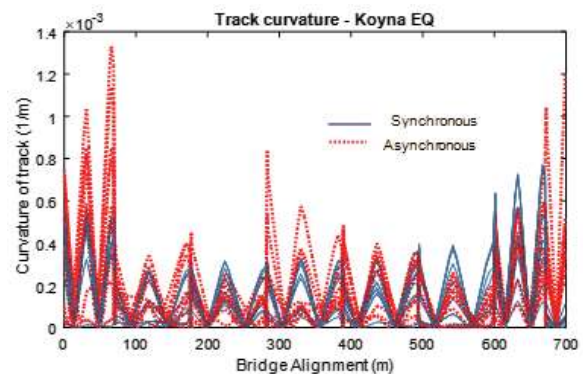
Fig. 10 Torsional Rotation Under El Centro Ground Motion

and node number 588 on span P1-P2, are considered for the study, which are rotational degree of freedom, i.e., torsion for the considered span. Figure 10 (a-b) clearly indicates that the torsion at those nodes is significantly higher for asynchronous and motion with wave passage effect than the similar values corresponding to the synchronous motion

get the deflected shape of the track. The boundary condition to form the spline is, the angle of rotation of the track at the two abutment ends is zero, as the track beyond the abutments may be considered as aligned along the bridge axis. The curvature of the deflected shape of the track has been calculated along the length of the bridge from the spline coordinates.

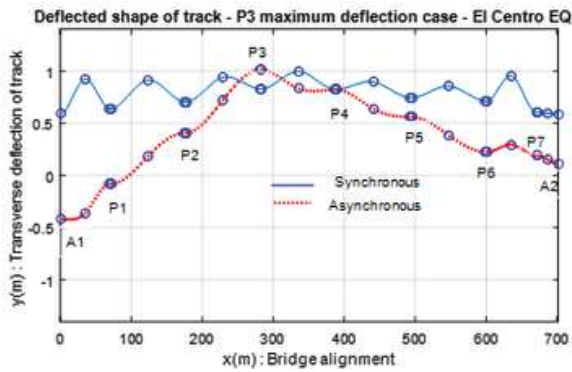


(a) Under Elcentro excitation

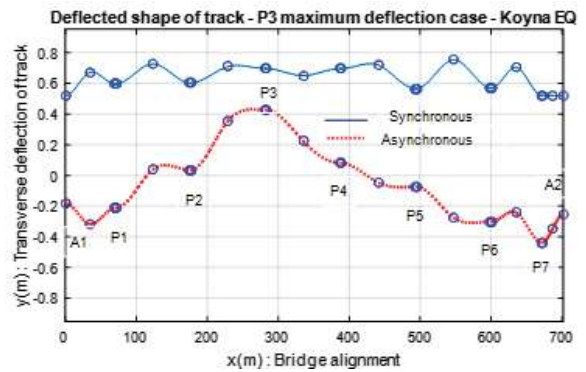


(b) Under Koyna excitation

Fig. 11 Track Curvature for Synchronous and Asynchronous Ground Motion



(a) Under Elcentro excitation



(b) Under Koyna excitation

Fig. 12 Deflected shape of track for synchronous and asynchronous transverse ground motion considering Koyna EQ at the time instance when P3 pier top undergoes maximum deflection.

Similar curvature of the deflected shape of the track has been calculated for other time instances when the other pier top deflections are maximum, and all these curvature plots have been superimposed in Fig. 9(a) for Elcentro EQ and in Figure 9(b) for Koyna EQ. The safe velocity of the train during EQ varies with the curvature of the track. More is the curvature, the less will be the safe velocity. From Figure 9 (a) the track curvatures are less in the case of asynchronous ground motion compared to synchronous ground motion, considering the El-Centro EQ. Whereas in Figure 9(b), considering Koyna EQ the trend is reversed. This shows that track curvature for asynchronous ground motion may be higher or lower compared to the synchronous ground motion for different EQ time histories.

5.5 Derailment factors for the assessment of safety

The running safety or derailment of trains over bridges during seismic events remains a key focus of ongoing train bridge interaction research. The risk of derailment is assessed indirectly using force-based criteria and displacement criteria as discussed in this section.

Nadal [19] first proposed the well-known force-based derailment criterion, based on the equilibrium between lateral (Y) and vertical forces (Q) at the wheel flange during static flange-climb conditions. Nadal’s formula for safety against derailment is given by:

$$\frac{Y}{Q} < \frac{\tan\beta - \mu}{1 + \mu \tan\beta}$$

where Y/Q is known as the derailment coefficient.

Although several authors have proposed modifications to Nadal’s formula over the years, its simplicity has made it the most widely used formula in derailment investigations. Due to its conservative estimation of the Y / Q ratio, it is well-suited for ensuring safety. On the railways, a flange slope of 2.5:1 ($\tan \beta = 2.5$ or $\beta = 68^{\circ}12'$) is typically used for the new wheel profile of carriages and wagons. Value of the coefficient of friction, μ depends on the geometry of the surfaces in contact, condition, and roughness of the surfaces, etc. On Indian Railways, μ in general is taken as 0.25. Thus, for $\beta = 68^{\circ}$ and $\mu = 0.25$, Right Hand Side of the Nadal equation works out to 1.4. This is the threshold value. To allow for a certain margin or factor of safety, a limiting value of 1.0 for the ratio Y / Q has been laid down on the Indian Railways, as one of the criteria for assessment of rolling stock stability. (“out of white metal of the - Yumpu”)

In addition to the force-based derailment criterion, displacement criteria based on the geometry of the wheel can also be used to check the stability of trains (Nishimura et al. [20], Tanabe et al. [21], Jin et al. [22]). The derailment is said to occur when the wheel lifts vertically to flange height (28.5 mm) and laterally slides from the initial regular position (63.5mm) as shown in Fig. 13.

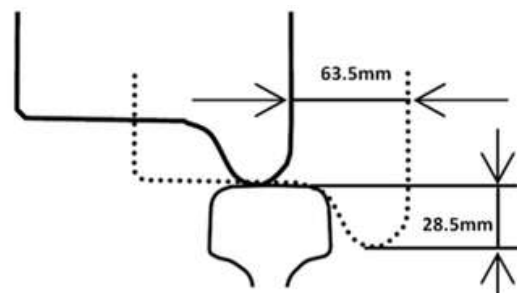


Fig. 13 Displacement Criteria for Derailment

From the analysis using train speed up to 120 kmph and corresponding to two different earthquakes, it has been found that the maximum value of the derailment coefficient is below 1.0. Similarly, both the vertical and lateral displacements are also below the limiting values. This trend has been observed considering both the synchronous and asynchronous ground motion.

6 Conclusions.

A long-span bridge with through type truss girder is considered for the analysis under simultaneous action of earthquake excitation and moving train. Finite element model of the bridge is made along with SSI using 1D nonlinear uncoupled springs. The bridge model is analysed using synchronous and asynchronous ground motions, and the responses of the bridge with a train moving at different speeds are studied. The responses of the Pier and deck are observed along with the relative displacement of adjacent piers. However, the derailment coefficient and displacement criteria revealed that the running train will remain safe for the input design spectrum compatible earthquake excitations considered.

The important conclusions are as follows:

- Increase in the displacement demand in piers and abutments is observed for the analysis with asynchronous input as compared to synchronous input-based analysis.
- Coherency losses in input motion may result in unseating of the superstructure due to larger relative displacement of adjacent piers.
- Active rotational degree of freedom that may lead to higher torsion in the superstructure, which is not found insignificant in the synchronous motion-based analysis.
- Effect of curvature in the track due to synchronous motion and asynchronous motion is case sensitive and depends on the characteristics of the ground motion itself.
- Bridge structure shows lesser displacement as well as acceleration response with a train on the bridge as compared to the case without train.

References

- [1] S.Adanur, A.C.Altunisik, H.B. Başıağa, K.Soyluk, A.A. Dumanoglu, "Wavepassage effect on the seismic response of suspension bridges considering local soil conditions," *Int. J. Steel Struct.*, 17(2), 501–513, 2017.
- [2] K. Konakli, A.D. Kiureghian, "Simulation of spatially varying ground motions including incoherence, wave-passage and differential site - response effects," *Earthq. Eng. Struct. Dyn.*, 41, 495–513, 2012.
- [3] J.L. Bogdanoff, J.E. Goldberg, A.J. Schiff, "The effect of ground transmission time on the response of long structures", *Bull. Seismol. Soc. America*, 55, 627–640, 1965.
- [4] A. Zerva, V. Zervas, "Spatial variation of seismic ground motions: An overview", *Applied Mechanics Reviews*, 55, 271–296, 2002.
- [5] D.I. Lavorato, I. Vanzi, C. Nuti, G. Monti. 2017. "Generation of non-synchronous earthquake signals", *Springer Series in Reliability Engineering*, in: Paolo Gardoni (ed.), *Risk and Reliability Analysis: Theory and Applications*, pages 169-198, Springer, 2017.
- [6] D. Basu , Rodda Gopala Krishnan, "Spatial variation and conditional simulation of seismic ground motion", *Bull Earthquake Eng.*, 16, 4399-4426, 2017.
- [7] K. M. Berrah, "A modal combination rule for spatially varying", *Earthq. Eng. Struct. Dyn.*, 22, 791–800, 1993.
- [8] A.D.E.R.Kiureghian, A.Neuenhofer, "Response spectrum method for multisupport seismic excitations," *Earthq. Eng. Struct. Dyn.*, 21, 713–740, 1992.

- [9] H. Mirzabozorg, M. Akbari, M.A. Hariri-Ardebili, "Nonlinear seismic response of a concrete arch dam to spatially varying earthquake ground motions," *Asian J. Civil Eng.* 14(6), 859–879, 2013.
- [10] Y. H. Zhang, Q. S. Li, J. H. Lin, F. W. Williams, "Random vibration analysis of long-span structures subjected to spatially varying ground motions," *Soil Dyn. Earthq. Eng.*, 29, 620–629, 2009.
- [11] K. Balamonica., N. Gopalakrishnan, A. Ramamohan Rao, "Seismic Analysis of Structures Subjected to Spatially Varying Earthquake Using POD Vectors: Experimental and Analytical Studies", *Journal of Earthquake and Tsunami*, 14(4), 2050017, 2020.
- [12] Bo Li, Kaiming Bi, Nawawi Chouw, John W. Butterworth, Hong Hao, "Experimental investigation of spatially varying ground motions on bridge pounding," *Earthq. Eng. Struct. Dyn.* 41, 1959–1976, 2012.
- [13] Nguyen, D. V., Kim, K. D., & Warnitchai, P. (2009). Simulation procedure for vehicle–substructure dynamic interactions and wheel movements using linearized wheel–rail interfaces. *Finite Elements in Analysis and Design*, 45(5), 341-356.
- [14] Yang, Y. B., Yau, J. D., Yao, Z., & Wu, Y. S. (2004). *Vehicle-bridge interaction dynamics: with applications to high-speed railways*. World Scientific.
- [15] American Petroleum Institute (API), "Recommended Practice for Planning, Designing and Constructing Fixed Offshore Platforms-Working Stress Design", API Publishing Services: Washington, DC, USA, 2000.
- [16] Computers and Structures, Inc. (CSI), "CSI Analysis Reference Manual for SAP2000", Berkeley, CA, 2009.
- [17] IS 1893, "Criteria for Earthquake Resistant Design of Structures- code of practice", New Delhi, 2016.
- [18] G. Fenton, E. H. A. Vanmarcke, "Conditioned simulation of local fields of earthquake ground motion", *Structural Safety*, 10, 247–264, 1991.
- [19] Nadal, M. J. (1896). *Théorie de la stabilité des locomotives, Part 2: Mouvement de lacet*. *Annales des Mines*, 10, 232
- [20] Nishimura, K., Terumichi, Y., Morimura, T., & Sogabe, K. (2010). Analytical study on the safety of high-speed railway vehicle on excited tracks. *Journal of System Design and Dynamics*, 4(1), 211-225.
- [21] Tanabe, M., Wakui, H., Sogabe, M., Matsumoto, N., & Tanabe, Y. (2011). An efficient numerical model for dynamic interaction of high-speed train and railway structure including post-derailment during an earthquake. In *8th International Conference on Structural Dynamics, EUROLYN*.
- [22] Jin, Z., Pei, S., Li, X., Liu, H., & Qiang, S. (2016). Effect of vertical ground motion on earthquake-induced derailment of railway vehicles over simply supported bridges. *Journal of Sound and Vibration*, 383, 277-294.

Authors



Abhishek,
Post Graduate Student,
Civil Engng. Dept., IIT
Guwahati, India



Prinza Priya Loying,
Research Scholar,
Civil Engng. Dept.,
IIT Guwahati, India



Sumantra Sengupta,
Research Scholar, Civil
Engng. Dept., IIT Guwahati,
India



Dr. Anjan Dutta,
Professor, Civil Engng.
Dept., IIT Guwahati,
India